The Journal of Immunology

RESEARCH ARTICLE | AUGUST 15 2017

Near-Infrared 1064 nm Laser Modulates Migratory Dendritic Cells To Augment the Immune Response to Intradermal Influenza Vaccine FREE

Kaitlyn Morse; ... et. al

J Immunol (2017) 199 (4): 1319–1332.
https://doi.org/10.4049/jimmunol.1601873

Near-Infrared 1064 nm Laser Modulates Migratory Dendritic Cells To Augment the Immune Response to Intradermal Influenza Vaccine

Kaitlyn Morse,* Yoshifumi Kimizuka,* Megan P. K. Chan,* Mai Shibata,* Yusuke Shimaoka,* Shu Takeuchi,* Benjamin Forbes,* Christopher Nirschl,[†] Binghao Li,* Yang Zeng,* Roderick T. Bronson,[‡] Wataru Katagiri,[§] Ayako Shigeta,* Ruxandra F. Sîrbulescu,* Huabiao Chen,* Rhea Y. Y. Tan,* Kosuke Tsukada,[§] Timothy Brauns,* Jeffrey Gelfand,* Ann Sluder,* Joseph J. Locascio,[¶] Mark C. Poznansky,*[,1] Niroshana Anandasabapathy,[†,1] and Satoshi Kashiwagi*

Brief exposure of skin to near-infrared (NIR) laser light has been shown to augment the immune response to intradermal vaccination and thus act as an immunologic adjuvant. Although evidence indicates that the NIR laser adjuvant has the capacity to activate innate subsets including dendritic cells (DCs) in skin as conventional adjuvants do, the precise immunological mechanism by which the NIR laser adjuvant acts is largely unknown. In this study we sought to identify the cellular target of the NIR laser adjuvant by using an established mouse model of intradermal influenza vaccination and examining the alteration of responses resulting from genetic ablation of specific DC populations. We found that a continuous wave (CW) NIR laser adjuvant broadly modulates migratory DC (migDC) populations, specifically increasing and activating the Lang$^+$ and CD11b$^-$Lang$^-$ subsets in skin, and that the Ab responses augmented by the CW NIR laser are dependent on DC subsets expressing CCR2 and Langerin. In comparison, a pulsed wave NIR laser adjuvant showed limited effects on the migDC subsets. Our vaccination study demonstrated that the efficacy of the CW NIR laser is significantly better than that of the pulsed wave laser, indicating that the CW NIR laser offers a desirable immunostimulatory microenvironment for migDCs. These results demonstrate the unique ability of the NIR laser adjuvant to selectively target specific migDC populations in skin depending on its parameters, and highlight the importance of optimization of laser parameters for desirable immune protection induced by an NIR laser–adjuvanted vaccine. ***The Journal of Immunology*****, 2017, 199: 1319–1332.**

The development of safe and potent immunologic adjuvants is a key challenge for vaccine progress. Typically, chemical or biological adjuvants are used to enhance vaccine efficacy, but most of these elicit side effects, including undesirable local reactogenicity or systemic toxicity due to their ability to stimulate innate immunity. These side effects may prevent approval for clinical use (1–3). An alternative to standard adjuvants is to stimulate the skin with laser light before an intradermally (i.d.) delivered vaccine. We have shown that briefly treating the skin vaccination site with a low-power, continuous wave (CW) 1064 nm near-infrared (NIR) laser light immediately before intradermal influenza vaccination significantly enhances immune responses, and results in improved survival in a lethal challenge murine influenza model (4). NIR laser exposures, unlike chemical or biological forms of conventional adjuvants, do not induce prolonged activation of innate immune responses, and the effects

*Vaccine and Immunotherapy Center, Division of Infectious Diseases, Department of Medicine, Massachusetts General Hospital, Charlestown, MA 02129; [†]Department of Dermatology, Harvard Skin Disease Research Center, Brigham and Women's Hospital, Boston, MA 02115; [‡]Department of Pathology, Harvard Medical School, Boston, MA 02115; [§]Graduate School of Fundamental Science and Technology, Keio University, Yokohama, Kanagawa 223-8522, Japan; and [¶]Alzheimer's Disease Research Center, Department of Neurology and Psychiatry, Massachusetts General Hospital, Boston, MA 02114

[1]M.C.P. and N.A. contributed equally to this work.

ORCIDs: 0000-0002-3077-2832 (K.M.); 0000-0002-6274-9485 (S.T.); 0000-0002-7333-2757 (C.N.); 0000-0001-7905-1713 (R.F.S.); 0000-0002-4056-9205 (R.Y.Y.T.); 0000-0002-2161-551X (T.B.); 0000-0002-4118-5676 (J.G.); 0000-0003-3439-1209 (J.J.L.); 0000-0002-0473-8358 (N.A.).

Received for publication November 2, 2016. Accepted for publication June 13, 2017.

This work was supported by the National Institute of Allergy and Infectious Diseases of the National Institutes of Health under award numbers R41AI114012, R42AI114012, and R01AI105131 (to S.K.), the Kanae Foundation for the Promotion of Medical Science (to Y.K.), the Mochida Memorial Foundation for Medical and Pharmaceutical Research (to Y.K.), the Uehara Memorial Foundation (to Y.K.), the Japan Foundation for Pediatric Research (to Y.K.), and the VIC Innovation Fund (to S.K.).

K.M. performed most of the experiments; K.M., Y.K., M.P.K.C., M.S., Y.S., S.T., B.L., Y.Z., A. Shigeta, R.F.S., and S.K. performed vaccination studies; K.M., Y.K., M.P.K.C., Y.S., and S.T. performed immunoassays; K.M. and S.K. designed most of the experiments; K.M., C.N., Y.K., M.P.K.C., Y.S., S.T., H.C., R.F.S., B.F., and R.Y.Y.T. contributed to the establishment of the animal model and immunoassays; R.T.B., Y.K., K.T., and W.K. performed the skin damage study; C.N. and N.A. contributed to analysis and experimental design related to the dendritic cell study; J.J.L. performed statistical analysis on Ab responses and advised on statistical tests in this study; K.M. and S.K. designed the study; K.M., T.B., J.G., M.C.P., A. Sluder, N.A., and S.K. analyzed the data; and K.M., N.A., M.C.P., A. Sluder, and S.K. wrote the manuscript.

The funders had no role in study design, data collection and analysis, the decision to publish, or preparation of the manuscript.

Address correspondence and reprint requests to Dr. Satoshi Kashiwagi, Vaccine and Immunotherapy Center, Division of Infectious Diseases, Department of Medicine, Massachusetts General Hospital, Room 5.239, 149 13th Street, Charlestown, MA 02129. E-mail address: skashiwagi@mgh.harvard.edu

The online version of this article contains supplemental material.

Abbreviations used in this article: cDC, classical lymph node–resident DC; CI, confidence interval; CW, continuous wave; DC, dendritic cell; dLN, draining LN; DT, diphtheria toxin; DTR, DT receptor; EID_{50}, 50% egg infectious dose; HAI, hemagglutination inhibition; i.d., intradermally; LN, lymph node; migDC, migratory DC; NIR, near-infrared; pDC, plasmacytoid DC; PW, pulsed wave; WT, wild type.

typically resolve within 24 h in exposed tissue (4). This suggests that NIR laser adjuvants have a distinct mechanism of action compared with chemical and biological adjuvants, and may have a more favorable safety profile while maintaining efficacy (4–6).

Multiple mechanisms of action have been described for clinical adjuvants, including establishment of an Ag depot effect, induction of inflammatory cytokines, activation of APCs, recruitment of innate immune cells, and facilitating Ag translocation to draining lymph nodes (dLNs) (7, 8). Although the specific mechanism by which the employed adjuvant enhances protective immunity in many vaccines is often unclear, an in-depth understanding of various adjuvant mechanisms of action is critical for establishing optimal adjuvant-vaccine formulations for induction of effective immunity against infections. Recruitment, activation, and maturation of dendritic cells (DCs) appears to play a central role in enhancing adaptive immunity. DCs are critical for the development of innate and adaptive immune responses against pathogens (9). DCs specialize in Ag presentation, directing T cell and humoral immune responses, and maintaining memory responses. An accumulating body of evidence demonstrates that different DC subsets are responsible for specialized immune functions. DCs imprint naive responses to direct the differentiation of CD4 helper T cells into T_H type 1 (T_H1), T_H2, T_H17, T follicular helper cells, type 1 regulatory T cells, and regulatory T cells (9–14). Multiple specialized subtypes of DCs that have been identified can be distinguished by surface markers, which have recently been correlated to their unique transcriptome-based programs across mice and humans (15–21).

Various types of clinical lasers can induce an immunostimulatory microenvironment that recruits and activates DCs, similar to that induced by classical chemical and biological adjuvants (5, 6). Wang et al. (22, 23) demonstrated that treatment of the vaccine inoculation site on the skin with a commercial nonablative fractional laser followed by intradermal vaccination augmented humoral immune responses, and induced cross-protective immunity in a lethal challenge murine model of influenza. Dying skin cells killed by laser release damage-associated molecular patterns, attracting APCs, in particular plasmacytoid DCs (pDCs), and resulting in augmentation of immune responses. Terhorst et al. (24) observed that skin micropores generated by ablative fractional lasers using the Precise Laser Epidermal System device enhanced the antitumor immune responses induced by prophylactic and therapeutic cancer vaccines. The local inflammatory milieu created by the death of keratinocytes during skin laser microporation was similarly responsible for activation of $XCR1^+$ DCs, thereby inducing tumor Ag-specific $CD8^+$ and $CD4^+$ T cell responses. We and others demonstrated that application of nontissue damaging lasers in skin also induces an immunostimulatory microenvironment that activates DCs (6, 25). The application of a pulsed wave (PW) 532 nm laser increases the motility of APCs in skin and increases Ag-positive $CD11c^+$ DCs in the skin-dLN (26), augmenting an anti-influenza T_H1-skewed immunity, resulting in suboptimal protection (4). We also previously noted that exposure to a low-power, CW 1064 nm NIR laser induced an upregulation of a selective set of chemokines in skin, accumulation of $CD11c^+$ cells and activation of DCs in skin-dLN, resulting in significant enhancement of immune responses and improved survival in a lethal influenza challenge murine model (4). However, in vivo cellular immunological responses to NIR laser adjuvants, including identification of the DC subsets that generate the distinct immune response to each laser, remain poorly characterized. A more precise description of these responses is needed to optimize the design of an adjuvanted vaccine incorporating the NIR laser to induce effective protection. In this study we show that the NIR lasers target specific DC subsets and augment immune responses to an influenza vaccine. These findings advance our mechanistic understanding of the combination of vaccine and laser adjuvant.

Materials and Methods

Animals

Female 6–8 wk old C57BL/6 mice (stock number 000664) were purchased from the Jackson Laboratory. All animals were acclimated for 2 wk prior to the beginning of the experiments. $CCR2^{-/-}$ (004999), $CCR7^{-/-}$ (006621), and Lang-GFP/diphtheria toxin receptor (DTR) (016940) mice were purchased from the Jackson Laboratory and bred at Massachusetts General Hospital. All animal procedures were performed following the Public Health Service Policy on Humane Care of Laboratory Animals and approved by the Institutional Animal Care and Use Committee of Massachusetts General Hospital.

Systemic depletion of cells harboring diphtheria toxin receptor

Langerin-GFP/DTR animals were injected i.p. with 4 ng/g diphtheria toxin (DT; Sigma-Aldrich) 24 h before immunization as described previously (27, 28). Control C57BL/6 mice were also treated with 4 ng/g DT within the same experiment.

Skin damage study

For visual inspection, we observed for any signs of skin damage including blistering, bruising, crusting, edema, redness, or swelling at 0, 1, 2, and 4 d after laser illumination as previously described (4). For skin histology, mice were heart-perfused with 4% paraformaldehyde before, or at 2, 6, and 24 h after laser illumination. Paraffin-embedded sections 5 μm thick were H&E stained and examined for microscopic tissue damage, and polymorphonuclear infiltration was quantitated on the slides in five randomized fields using ImageJ freeware (National Institutes of Health) as previously described (4).

Laser adjuvant illumination and influenza vaccinations

An Nd:YVO_4 1064 nm laser (RMI laser, Lafayette, CO) was used as previously described (4). The 1064 nm laser can be set to emit either CW or nanosecond PW at a repetition rate of 10 kHz. The irradiance (power density) of both the CW and PW 1064 nm lasers at the skin surface was 5 W/cm^2, as this irradiance was shown previously to be non-tissue damaging over an extended period of time, to maintain skin temperature $<43^{\circ}C$, and to induce optimal adjuvant effects (4). The 532 nm laser output was PW only at 10 kHz at an irradiance of 1 W/cm^2. All lasers were adjusted to illuminate a circular exposure on the skin of ~5 mm (0.2 cm^2) with less than a 50% difference in beam intensity from center to edge. Laser exposures at 1064 nm were 1 min with a total dose of 300 J/cm^2, and at 532 nm were 4 min with a total dose 240 J/cm^2.

Mice were depilated (Nair; Church & Dwight) 2–3 d before laser adjuvant illumination and immunization. The inactivated influenza virus A/PR/8/34 (H1N1; Charles River) vaccine was delivered i.d. using 1 μg in a total volume of 10 μl of saline per mouse. Vaccine was injected in the center of the laser-treated spot on the back of the mouse within 5 min of the laser treatment. Vaccination groups included: no vaccine (saline or sham treated), 1 μg vaccine only, CW 1064 nm illuminated for 1 min at 5 W/cm^2 prior to 1 μg i.d. vaccine, PW 1064 nm illuminated for 1 min at 5 W/cm^2 followed by 1 μg i.d., PW 532 nm laser illuminated for 4 min at 1 W/cm^2 followed by 1 μg i.d., 1 μg influenza vaccine delivered i.m., 1 μg influenza vaccine mixed with alum (Imject; Thermo Fisher) delivered i.d., and 1 μg influenza vaccine mixed with an oil-in-water emulsion adjuvant with a formulation similar to MF59 (AddaVax; InvivoGen) delivered i.d. As described previously, 28 d later mice were homologously challenged intranasally with live A/PR/8/34 (H1N1) virus at a dose of 2×10^5 50% egg infectious doses (EID_{50}). Four days after challenge, mice were sacrificed and blood and spleen samples were taken for further analysis (4).

Anti-influenza Ab responses and determination of hemagglutination inhibition titers

Anti-influenza IgG, IgG1, and IgG2c humoral responses were measured by ELISA as previously described (4). Briefly, ELISA plates (Immulon) were coated with 100 ng of inactivated influenza virus. Serially diluted mouse serum samples were added to the wells, and bound Igs were detected with the appropriate secondary Ab (goat anti-mouse IgG [1:10,000; Sigma-Aldrich], rat anti-mouse IgG1 [1:2000; SouthernBiotech], or goat anti-mouse IgG2c [1:4000; SouthernBiotech]). A titer was designated as the

serum dilution corresponding to the inflection point of the plot of the OD versus dilution of serum. Hemagglutination inhibition (HAI) titers in sera samples were determined by SRI International (Harrisburg, VA).

Assessment of T cell responses

Splenocytes were harvested 4 d post live influenza challenge and immediately processed for assessment of T cell responses. Splenocyte preparations were each divided into two duplicate wells within a round-bottom 96-well plate containing 1×10^6 cells, and incubated with or without 1 μg/ml inactive influenza for 60 h for determination of cytokine release from splenocytes. Splenocyte culture supernatants were collected and the amounts of IFN-γ or IL-4 (picograms per milliliter) were determined using DuoSet ELISA kits (R&D Systems) following the manufacturer's instructions.

Influenza virus challenge study

Immunized mice were anesthetized and challenged intranasally with live influenza A/PR/8/34 at a dose of 1.5×10^6 EID_{50}, which is equivalent to $150 \times 50\%$ mouse lethal dose, in 30 μl saline 28 d after vaccination as previously described (4). Survival and body weight were monitored for 15 d postchallenge. Mice showing a hunched posture, ruffled fur, or >20% body weight loss, or mice that were not eating or drinking, were considered to have reached the experimental endpoint.

Immunization with OVA and DC isolation from lymph nodes

To quantitate DC migration and function in vivo, mice were injected i.d. with a total of 40 μg of endotoxin-free OVA conjugated to Alexa Fluor 488 (OVA-A488) (Life Technologies) as described previously (4). Briefly, the prepared mouse back was illuminated with the NIR laser in four locations, as described above. This was followed by i.d. injections of OVA-A488 at each treatment site (10 μg in 10 μl saline per spot, four spots in total).

To quantify DC subsets, skin-dLN (inguinal, brachial, and axial) were harvested and pooled from each animal 24 h after laser administration and OVA-A488 injections. Lymph nodes (LNs) were teased apart and incubated with collagenase D (2.5 mg/ml and 0.45 U/ml; Roche) at 37˚C for 25 min in HBSS (Invitrogen). Then 10 mM EDTA was added for an additional 5 min incubation as previously described (29). Five million cells per well were plated for subsequent labeling for flow cytometry.

Subtyping of DCs in LNs by flow cytometry

Cells isolated from skin-dLN were labeled on ice in 2–5% FBS/PBS using the Cytofix/Cytoperm kit (BD Biosciences) for multiparameter flow cytometry. The following Abs were obtained from BD, eBioscience, or BioLegend: hamster anti-mouse CD11c (PE; N418), rat anti-mouse MHC class II (I-A/I-E) (A700; M5/114.15.2), rat anti-mouse CD11b (PerCP Cy5.5; M1/70), hamster anti-mouse CD103 (PE Cy7; 2E7), mouse anti-mouse langerin (CD207) (APC; 4C7), rat anti-mouse CD8a (APC e780, 53-6.7), and rat anti-mouse CD86 (BV605; GL1). Live/dead aqua and OVA conjugated to A488 were obtained from Life Technologies. Data acquisition was performed on a Fortessa cytometer (BD; four lasers, capable of acquiring 13 colors, DIVA software for automatic compensation) followed by analysis on FlowJo software (Tree Star).

DC subsets from dLN were gated similarly to a previous description (29) using the following strategy: scatter, exclusion of dead cells, singlets, and $CD11c^+$ versus MHC class II. Classical LN–resident DCs (cDC) were selected on $CD11c^{hi}$ status and I-A/I-E intermediate levels, and were further subgated for $CD11b^+$ versus $CD103^+$ populations. Migratory DCs (migDCs) were selected for CD11c intermediate levels and I-A/I-E^{hi} status as distinct from cDC, and further gated for Langerin ($Lang^+$) versus $CD11b^+$. From cells within the $migDC^+$ $Lang^+$ gate, $CD11b^+$ versus $CD103^+$ subpopulations were further gated (Supplemental Fig. 1).

Cutaneous FITC painting assay

Mice were shaved and depilated as described above. Four hours prior to the intradermal vaccination and laser treatment, mice were painted on the four spots of flank back skin (~5 mm in diameter per spot) with 10 μl of a 1% FITC solution (Isomer I; Sigma) prepared in acetone:dibutyl phthalate (1:1, vol/vol; Sigma) as previously described (30). NIR laser treatment followed by vaccination with OVA (EndoFit OVA; InvivoGen) at each treatment site (10 μg in 10 μl saline per spot, four spots in total) was performed on the FITC-painted sites. We then harvested skin-dLN 24 and 48 h after the vaccination and laser treatment, isolated DCs from LN, and analyzed them using the same strategy as described above, on the basis of surface markers of DCs and FITC fluorescence by flow cytometry.

Statistical analyses

A log transformation of Ab titers was applied for Ab titer analysis to reduce positive skewing in the distribution of the raw Ab titers that would violate parametric test assumptions. We ran a mixed within- and between-subject (mouse) repeated measures ANOVA, where the three Ab titers of IgG and subclasses (IgG, IgG1, IgG2c) were treated as a three-level, within-subject factor, crossed with the between subject factors of four genotypes (wild type [WT], Lang-GFP/DTR, $CCR2^{-/-}$, $CCR7^{-/-}$) and three treatments (vaccine i.d., vaccine i.d. + CW 1064 nm, vaccine i.d. + PW 1064 nm). All two- and three-way interactions of within and between factors were included in the initial run. Nonsignificant terms were subsequently removed in a backward elimination algorithm using a cutoff of $p = 0.05$. The df were adjusted for correlated error with the Huynh–Feldt correction. Tukey post hoc multiple comparison tests were run as needed.

A similar analysis restricted to the WT genotype was also run crossing the three-level, within-subject Ab factor (IgG, IgG1, IgG2c) with the seven-level, between-subject treatment factor (vaccine i.d., vaccine i.d. + CW 1064 nm, vaccine i.d. + PW 1064 nm, vaccine i.d. + PW 532 nm, vaccine i.m., vaccine + alum i.d., and vaccine + MF59 i.d.). Because the IgG, IgG1, and IgG2c responses of WT mice injected with or without DT for all treatments were not statistically significant, we pooled the results within the same treatment groups.

For the assessment of T cell responses, a similar analysis was run where the two cytokines (IFN-γ, IL-4) were treated as a two-level, within-subject factor, crossed with the between-subject factors of four genotypes (WT, Lang-GFP/DTR, $CCR2^{-/-}$, $CCR7^{-/-}$) and three treatments (vaccine i.d., vaccine i.d. + CW 1064 nm, vaccine i.d. + PW 1064 nm). A similar analysis restricted to the WT genotype was also run crossing the two-level, within-subject cytokine factor (IFN-γ, IL-4) with the seven-level, between-subject treatment factor (vaccine i.d., vaccine i.d. + CW 1064 nm, vaccine i.d. + PW 1064 nm, vaccine i.d. + PW 532 nm, vaccine i.m., vaccine + alum i.d., and vaccine + MF59 i.d.).

For the assessment of CD86 expression, we normalized data on a scale of 0–1 to account for variations of signal intensity, instrumental settings, and fluorescence settings to pool the results generated by flow cytometry from multiple experiments. Data noted as relative median fluorescence were analyzed using nonparametric Kruskal–Wallis with Dunn correction for multiple comparisons.

The data analysis for this paper was conducted using SAS/STAT software for Windows (SAS Institute, Cary, NC) and Prism 6 (GraphPad software 2015). Data were pooled from at least two independent experiments for each treatment that was evaluated.

Results

Nanosecond-PW NIR laser is non-tissue damaging

We first determined if the previously established maximum dosage of the PW NIR laser (4) was non-tissue damaging, as it was not determined in the previous study. Mice received exposures at 5 W/cm^2 for 1 min, at which the maximum safe irradiance with no visual skin damage was confirmed and skin temperatures did not exceed 43˚C. Skin damage was evaluated after illumination by visual inspection and histology. No visual damage such as blistering, bruising, crusting, edema, redness, or swelling was seen at any time point for both the 1064 nm PW and CW laser (Supplemental Fig. 2A), which is consistent with our previous report (4). On histological examination, no tissue damage or inflammatory response at any given time point was detected by H&E staining (Supplemental Fig. 2B), as evidenced by minimal polymorphonuclear cell–infiltration in the skin (<6 per mm^2 on average, Supplemental Fig. 2C). Thus, we concluded that the dosage for the PW NIR laser was non-tissue damaging and non-inflammatory.

CW and PW 1064 nm lasers augment immune responses to influenza vaccination

We next compared the adjuvant effect of the PW NIR laser with previously explored visible and CW NIR lasers and conventional adjuvants including alum and an oil-in-water emulsion, AddaVax, in a murine influenza vaccination model. Mice received a single laser dose and were injected i.d. with whole inactivated influenza virus A/PR/8/34.

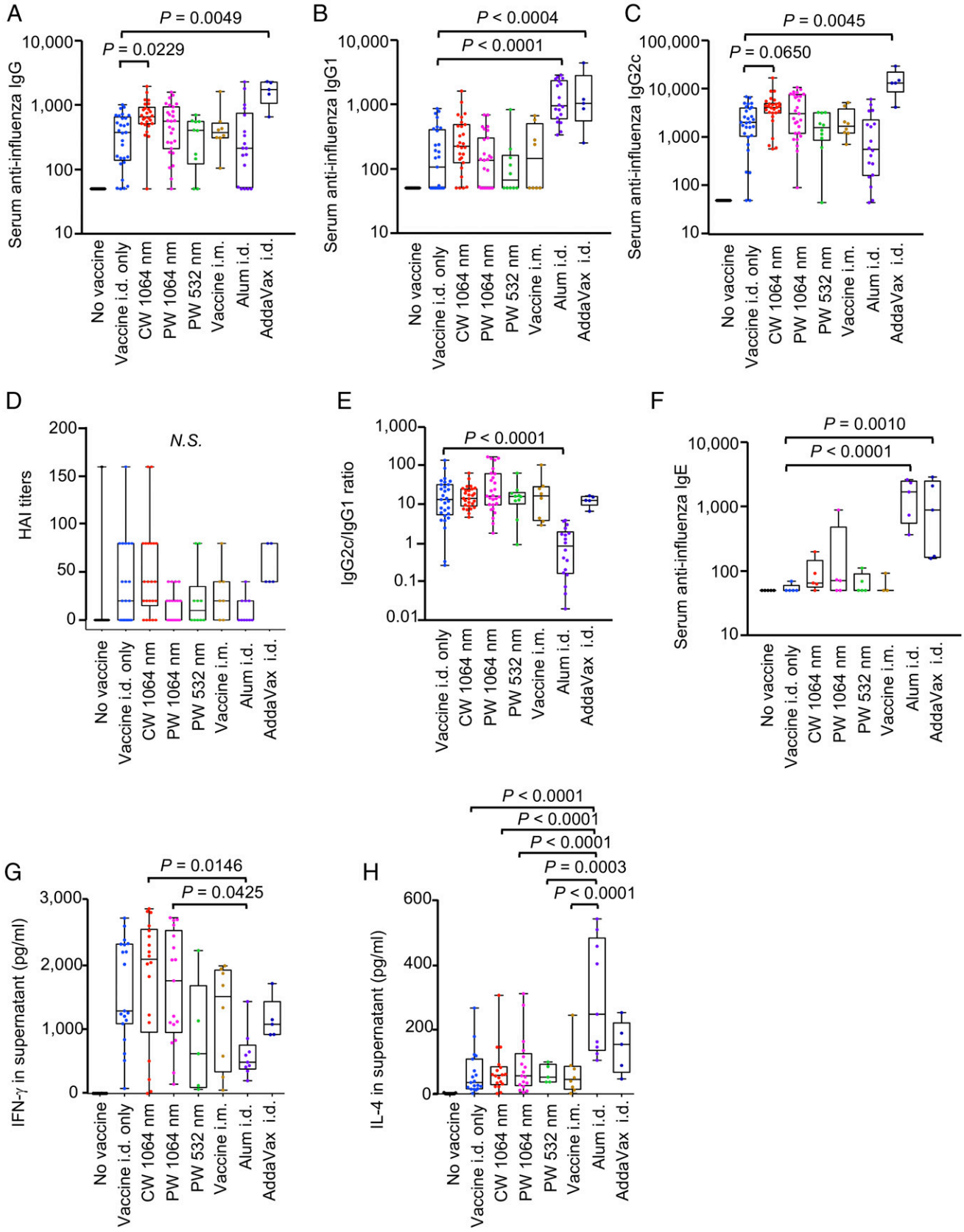

FIGURE 1. Effect of the laser adjuvant on anti-influenza immune responses. (**A**–**F**) Influenza-specific humoral responses 4 d after challenge. Mice were vaccinated with 1 μg of inactivated influenza virus (A/PR/8/34) with or without laser illumination or representative chemical adjuvant (alum or AddaVax) and challenged intranasally with live homologous virus 4 wk after vaccination. Titer of influenza-specific serum IgG subclass was determined by ELISA, plates were coated with inactivated influenza virus. (A) IgG, (B) IgG1, and (C) IgG2c titers. (D) HAI titers. (E) IgG2c/IgG1 ratio. (F) IgE titers. (**G** and **H**) Systemic T cell responses were measured 4 d after challenge by restimulating 1×10^6 splenocytes with inactivated influenza vaccine Ag. Levels of (G) IFN-γ and (H) IL-4 in splenocyte culture supernatants are shown. Experimental and control groups: (A–C and E) $n = 30, 29, 26,$ (*Figure legend continues*)

The CW NIR laser significantly augmented anti-influenza IgG response ($p = 0.0229$, Fig. 1A) and induced a statistically marginal increase in IgG2c ($p = 0.0650$, Fig. 1C) compared with the non-adjuvanted i.d. only group. The HAI geometric mean titer for the CW laser group was higher (20.25, 95% confidence interval [CI], 9.17–44.69) than that of the non-adjuvanted i.d. only group (8.484, 95% CI, 3.407–21.13), although this difference was not statistically significant (Fig. 1D). The CW laser adjuvant induced a similar anti-influenza IgG2c:IgG1 ratio (Fig. 1E) and IFN-γ and IL-4 secretion levels from ex vivo stimulated splenocytes compared with the nonadjuvanted i.d. only group (Fig. 1G, 1H). Our results confirm that the CW NIR laser adjuvants an influenza vaccine, inducing a mixed T_H1 and T_H2 immunity as previously reported (4). The PW laser adjuvant similarly augmented anti-influenza IgG titer (Fig. 1A–C) with no appreciable increase in HAI titer and a similar IgG2:IgG1 ratio (Fig. 1D) and IFN-γ and IL-4 secretion levels from ex vivo stimulated splenocytes (Fig. 1G, 1H) compared with the nonadjuvanted group (Fig. 1E). None of these observations were statistically significant. Taken together, these results suggest that the CW NIR laser is a more effective adjuvant than the PW laser for intradermal influenza vaccine.

We also compared the efficacy of the PW 532 nm green laser adjuvant as well as conventional adjuvants, alum and Addavax. In our current study, PW 532 nm laser administration produced neither significant anti-influenza Ab responses nor T cell responses (Fig. 1A–D, 1G, 1H), as previously reported (4). A mixture of influenza vaccine with alum resulted in elevated anti-influenza IgG1 ($p < 0.0001$, Fig. 1B), significantly lower IgG2:IgG1 ratio than the non-adjuvanted group ($p < 0.0001$, Fig. 1E), increased IL-4 ($p = 0.0006$, Fig. 1H) and decreased IFN-γ (Fig. 1G) influenza-specific responses compared with the non-adjuvanted group. The finding is consistent with published data showing that alum induces a profoundly polarized T_H2 response (8, 31). We also show that the alum adjuvant induces a significant anti-influenza IgE response (Fig. 1F, $p < 0.0001$ compared with the nonadjuvanted i.d. only group). A mixture of the influenza vaccine with Addavax, delivered i.d., significantly increased anti-influenza IgG, IgG1, and IgG2c responses (IgG: $p < 0.0049$, IgG1: $p = 0.0004$, IgG2c: $p < 0.0045$, Fig. 1A–C) with a similar IgG2:IgG1 ratio to the nonadjuvanted group (Fig. 1E). The HAI geometric mean titer for the Addavax group was the highest among the test groups (52.78, 95% CI, 32.94–84.57), although this difference is not statistically significant (Fig. 1D). However, Addavax generated a significantly increased IgE (Fig. 1F, $p = 0.0010$), resembling an allergic response. These results indicate that the use of chemical adjuvants, including Addavax, for i.d. vaccination may lead to unexpected induction of hypersensitivity. In contrast, NIR laser adjuvants, including the newly tested PW NIR laser, did not induce appreciable IgE responses (Fig. 1F). Together, these data indicate that NIR laser treatment produces a mixed T_H1–T_H2 immune response to influenza vaccination depending on laser parameter without inducing any hypersensitivity.

The NIR laser adjuvant modulates migDC population within the skin-dLN

We have shown that the CW NIR laser induces migrational and functional changes of $CD11c^+$ cells in skin and dLN (4). To further identify which specific DC subsets are activated by the CW and PW NIR laser adjuvants, we harvested skin-dLN 24 h after laser treatment and i.d. injection of fluorescently labeled OVA.

Tissue migDC in skin-dLN, defined by MHC class II^{hi}-$CD11c^{int}$ expression, can be further divided into the following functionally distinct subsets: $Langerin^-CD11b^-$, $Langerin^-CD11b^+$, $Langerin^+CD103^+CD11b^-$, and $Langerin^+CD103^-CD11b^+$ Langerhans cells (32–35). In addition to migDC, cDC that are resident within LN originate from the bone marrow. cDC are characterized by MHC-$II^{int}CD11c^{hi}$ expression and contain $CD11b^+$ ($CD8\alpha^-$) and $CD103^+$ ($CD8\alpha^+$) subsets. pDCs are characterized by MHC-II^{low} $CD11c^{low}$ expression and are capable of priming T cells postinfection or immunization in LN (36). The pDC, cDC, and migDC populations were evaluated as defined by their varying MHC class II and CD11c expression and their surface markers including Langerin, CD11b, and CD103 as previously described (29). The CW NIR laser adjuvant increased the number of migDC populations compared with the no laser-OVA i.d. only control group ($p = 0.0139$, Fig. 2A, 2B). These migDC were also preferentially activated by the CW NIR laser treatment, as indicated by the expression of CD86 ($p = 0.0483$, Fig. 2C, 2D). Among all the DC subsets in skin, $Lang^-CD11b^-$ DCs preferentially expanded following NIR CW laser illumination ($p < 0.0001$, Fig. 2E, 2F), accompanied by a marginal increase in $CD11b^+$ migDC subset (Fig. 2E, 2F). The NIR laser did not induce appreciable changes in the number of cDC or pDC in LN (Fig. 2A, 2B). Further analysis indicated that the CW NIR laser adjuvant induced no appreciable change in $Lang^+$ migDC (Fig. 2G, 2H) or the cDC subsets (Fig. 2I, 2J).

The PW NIR laser adjuvant did not induce appreciable changes in the number of migDC in LN (Fig. 2A, 2B), nor did it significantly alter the expression of activation markers of migDC subsets (Fig. 2C, 2D). The PW NIR laser adjuvant led to a marginal decrease in $Lang^+$ migDC subsets compared with OVA i.d. only group (Fig. 2E, 2F), while inducing no change in other DC subsets. Further analysis showed the PW NIR laser decreased the number of both $Lang^+$ $CD11b^+$ and $Lang^+CD103^+$ migDC subsets slightly as compared with OVA i.d. group (Fig. 2G, 2H), although this change is not statistically significant. The PW laser adjuvant did not significantly alter $CD11b^+$ or $CD103^+$ within cDCs subsets (Fig. 2I, 2J).

In our previous findings describing the CW NIR laser adjuvant, NIR laser illumination of the skin resulted in increased *ccl2* and *ccr2* gene expression in skin and an increase in the number of MHC class II^+ $CD11c^+$ DCs within the dLN 6 h after skin illumination with the laser (4). This led us to evaluate the recruitment of inflammatory monocytes and monocyte-derived DC (16, 37, 38) by the NIR laser adjuvant. The CW NIR laser adjuvant increased the number of $CD11b^+Ly6C^+$ monocytes in skin-dLN compared with the OVA i.d. only control group ($p = 0.0435$, Fig. 2K, 2L), whereas the PW NIR laser induced a statistically marginal increase in this population.

Together, these results suggest that the CW NIR laser adjuvant modulates $Lang^-CD11b^-$ migDCs and induces recruitment of $CD11b^+Ly6C^+$ monocytes, whereas the PW NIR laser adjuvant shows a marginal effect on these DC populations.

The NIR laser adjuvant activates an Ag-bearing migDC population within the skin-dLN

To further dissect the functional alteration of each DC subset induced by the NIR laser adjuvant, we analyzed the numerical and

27, 10, 8, 18, 5; (D) $n = 14, 22, 22, 22, 10, 7, 10, 5$; (F) $n = 5, 5, 5, 5, 5, 3, 5, 5$; (G and H) $n = 20, 19, 18, 17, 5, 8, 9, 5$, for no vaccine, vaccine i.d., vaccine i.d. + CW 1064 nm, vaccine i.d. + PW 1064 nm, vaccine i.d. + PW 532 nm, vaccine i.m., vaccine + alum i.d., and vaccine + AddaVax i.d. vaccine groups, respectively. Results were pooled from three independent experiments and analyzed using two-way ANOVA with Tukey correction.

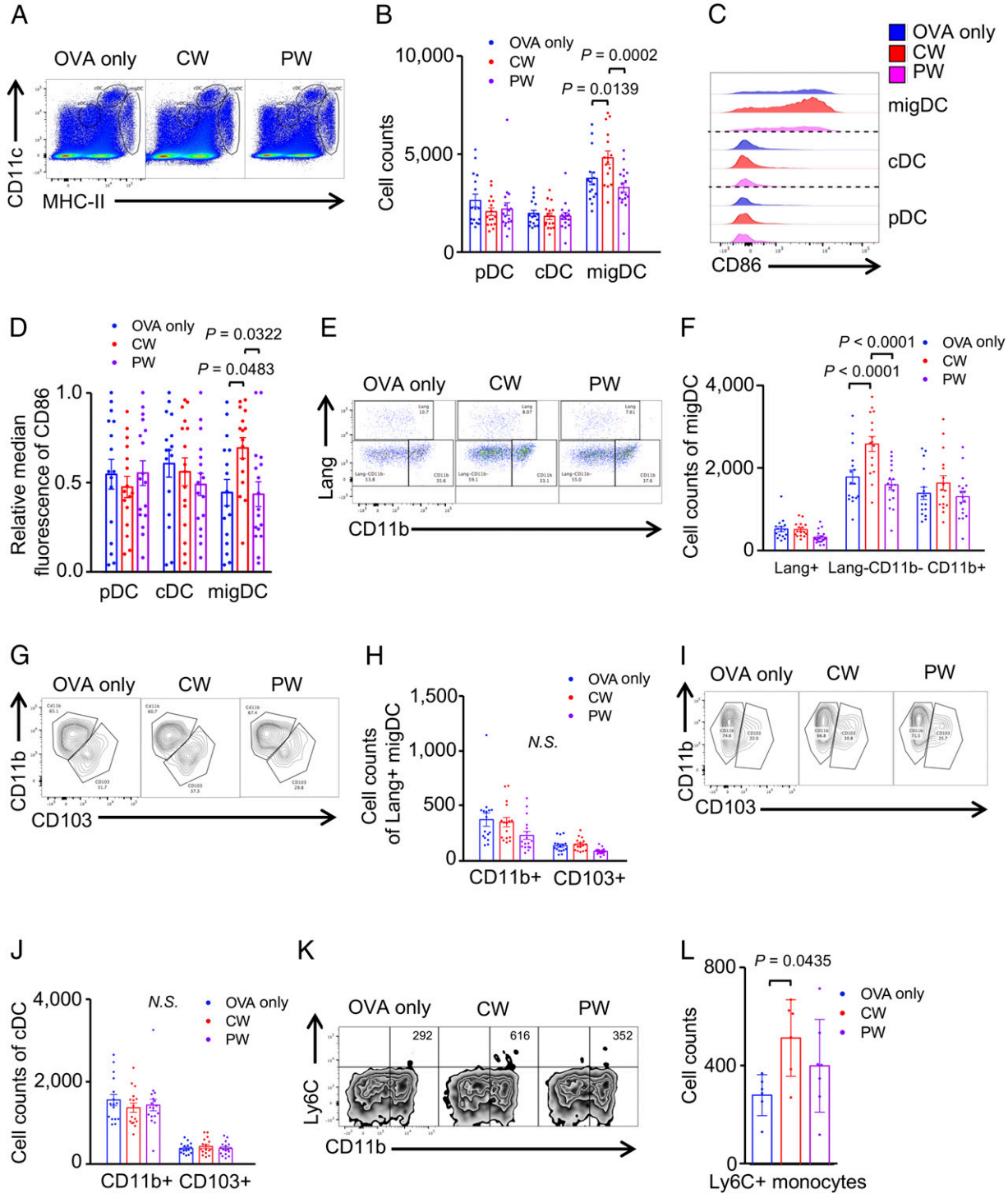

FIGURE 2. The effect of NIR laser adjuvant on DCs within the skin-dLN. DCs in skin-dLN were processed and stained for multiparameter flow cytometry 24 h after intradermal vaccination with 40 μg Alexa Fluor-488–labeled OVA with or without 1 min CW or PW 1064 nm NIR laser treatment. (**A**) Representative gates of pDC, cDCs, and migDC; numbers indicate percent of total lymphocytes. (**B**) Cell counts. (**C**) Representative histograms of CD86 expression. (**D**) Median fluorescence intensity of CD86 expression for pDC, cDC, and migDC population. (**E**) Representative gates of migDC subsets. (**F**) Cell counts of migDC subpopulation within skin-dLN. (**G**) Representative gates of Lang$^+$migDC subsets, numbers indicate percent of parent. (**H**) Cell counts of Lang$^+$migDC subpopulation within skin-dLN. (**I**) Representative gates of cDC subsets, number representing percent of parent. (**J**) Cell counts of cDC subpopulation within skin-dLN. (**K**) Representative gates of CD11b$^+$Ly6C$^+$ monocytes. (**L**) Cell counts of CD11b$^+$Ly6C$^+$ monocytes within skin-dLN. Data were analyzed with (B, F, H, J and L) two-way ANOVA followed by the Tukey honestly significant difference (HSD) tests or (D) Kruskal–Wallis with Dunn correction for multiple comparisons. Experimental and control groups: (A–J) n = 16, 16, 17; (K and L) n = 6, 6, 7, for OVA i.d., OVA i.d. + CW 1064 nm, OVA i.d. + PW 1064 nm, respectively. Data are derived from three independent experiments.

functional changes in Ag-bearing (OVA$^+$) cells in skin-dLN 24 h after laser treatment and i.d. injection of fluorescently labeled OVA.

The CW NIR laser induced a significant increase of the number of OVA$^+$ migDC in comparison with the no-laser OVA i.d. only control group (p = 0.0202, Fig. 3A, 3B). Across all the migDC

subsets, the NIR CW laser preferentially increased OVA uptake by Lang$^-$CD11b$^-$ migDCs and the number of OVA$^+$ Lang$^-$CD11b$^-$ migDCs, although this numerical increase is not statistically significant (Fig. 3C, 3D). Furthermore, the CW NIR laser induced a marginal increase of the number of OVA$^+$Lang$^+$CD11b$^+$migDC subset (Fig. 3E) in comparison with the no laser OVA i.d. only control group.

In contrast, mice treated with PW NIR laser adjuvant exhibited more OVA$^+$ cells, including CD11b$^+$, Lang$^+$CD11b$^+$ migDC subsets, whereas there were fewer OVA$^+$ cells in the Lang$^+$ CD103$^+$ migDC subset, as compared with the no-laser OVA i.d. only control group (Fig. 3C, 3D), although these changes were not statistically significant.

In short, these results are consistent with the view that the CW NIR laser adjuvant preferentially modulates Lang$^-$CD11b$^-$ migDCs, whereas the PW NIR laser adjuvant possibly modulates Lang$^+$ and CD11b$^+$ migDCs.

The CW NIR laser adjuvant augments migration of skin-resident migDC to the skin-dLN

Skin-resident migDCs constantly migrate into the skin-dLN in normal and inflammatory settings, orchestrating a wide array of adaptive immune responses (39). Our data consistently show that the NIR laser adjuvant selectively modulates migDCs in the skin-dLN. These findings led us to assess the effect of NIR laser adjuvant on migration of migDC subsets in skin. To this end, we used an established cutaneous FITC-painting assay to quantitate DC migration from skin to the skin-dLN (30). We applied FITC solution to the flank skin of mice prior to the NIR laser treatment followed by i.d. injection of OVA. We then assessed the migration of migDC subsets into the skin-dLN at 24 and 48 h after vaccination.

The CW NIR laser adjuvant increased the number of FITC$^+$ migDC populations compared with the no-laser OVA i.d. only control group (24 and 48 h, $p < 0.0001$), although near-background numbers of FITC$^+$ cDCs or pDCs were detected at these time points (Fig. 4A, 4B). Among all the DC subsets in skin, the NIR CW laser preferentially facilitated migration of Lang$^-$ CD11b$^-$ (24 h, $p = 0.0014$; 48 h, $p < 0.0001$) and Lang$^+$ (48 h, $p = 0.0084$) migDC subsets, as compared with no-laser OVA i.d. only control group (Fig. 4C, 4D). Further analysis revealed that the CW NIR laser marginally increases Lang$^+$CD103$^+$ and significantly increases Lang$^+$CD11b$^+$ DCs compared with no-laser OVA i.d. only control group (24 h, $p = 0.0134$; 48 h, $p = 0.0178$, Fig. 4E, 4F).

The PW laser adjuvant did not significantly alter the number of FITC$^+$ DCs within migDCs subsets in LN compared with no-laser OVA i.d. only control group (Fig. 4).

Because the CW NIR laser adjuvant most efficiently augments the arrival of FITC$^+$ migDCs to the skin-dLN and the corre-

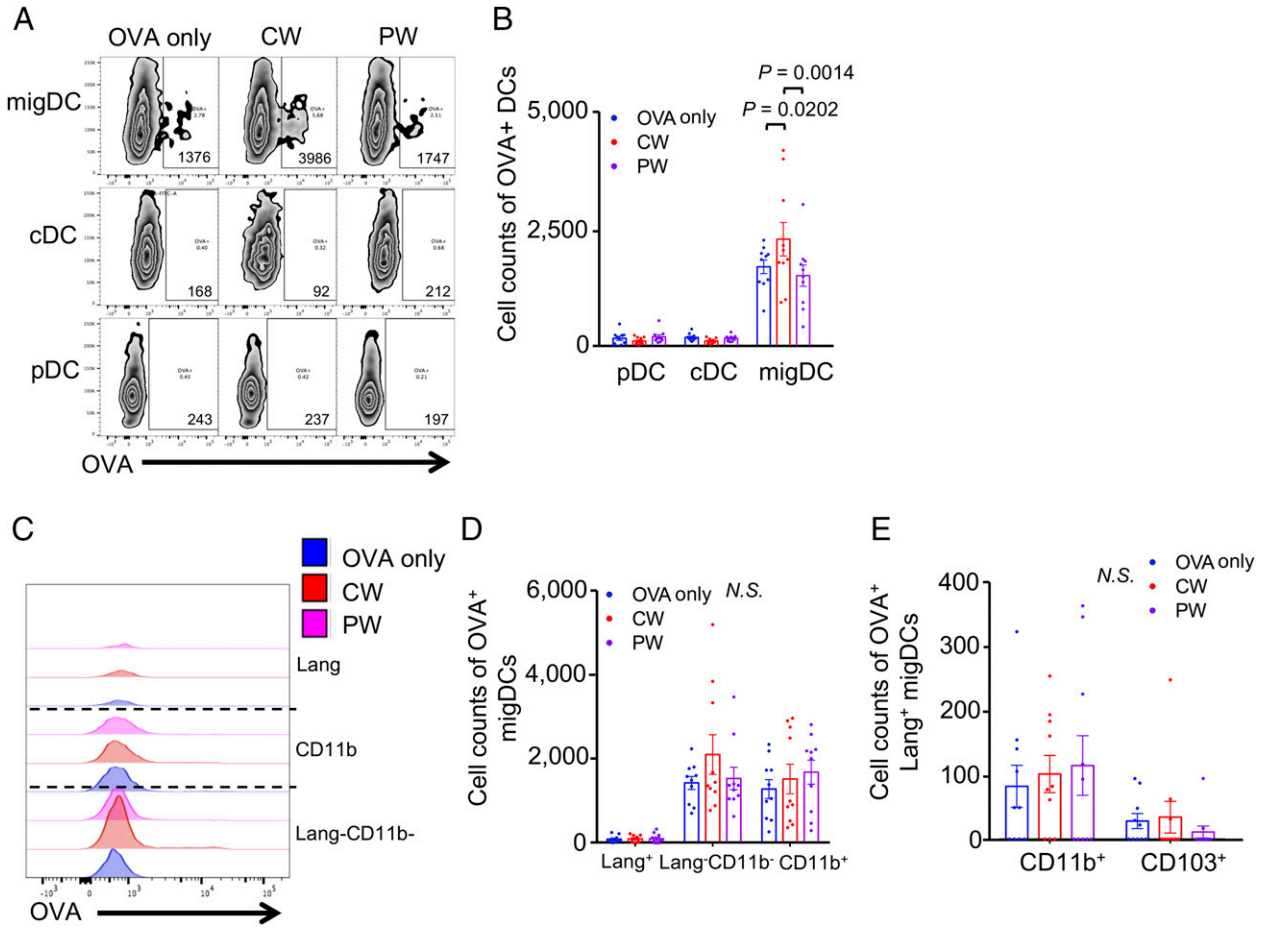

FIGURE 3. The effect of NIR laser adjuvant on Ag-bearing DCs within the skin -dLN. (**A**) Representative gates of pDC, cDC, and migDC bearing OVA Ag, number indicates cell count of positive gate. (**B**) Cell counts of OVA$^+$ pDC, cDC, and migDC populations within skin-dLN. (**C**) Representative histograms of OVA$^+$migDCs. (**D**) Cell counts of OVA$^+$migDC subpopulation within skin-dLN. (**E**) Cell counts of OVA$^+$Lang$^+$migDC subpopulation within skin-dLN. (B, D and E) Data were analyzed with two-way ANOVA followed by the Tukey honestly significant difference (HSD) tests. Experimental and control groups: (A–E) n = 15, 16, 16, 17 for no vaccine, OVA i.d., OVA i.d. + CW 1064 nm, OVA i.d. + PW 1064 nm, respectively. Data are derived from three independent experiments.

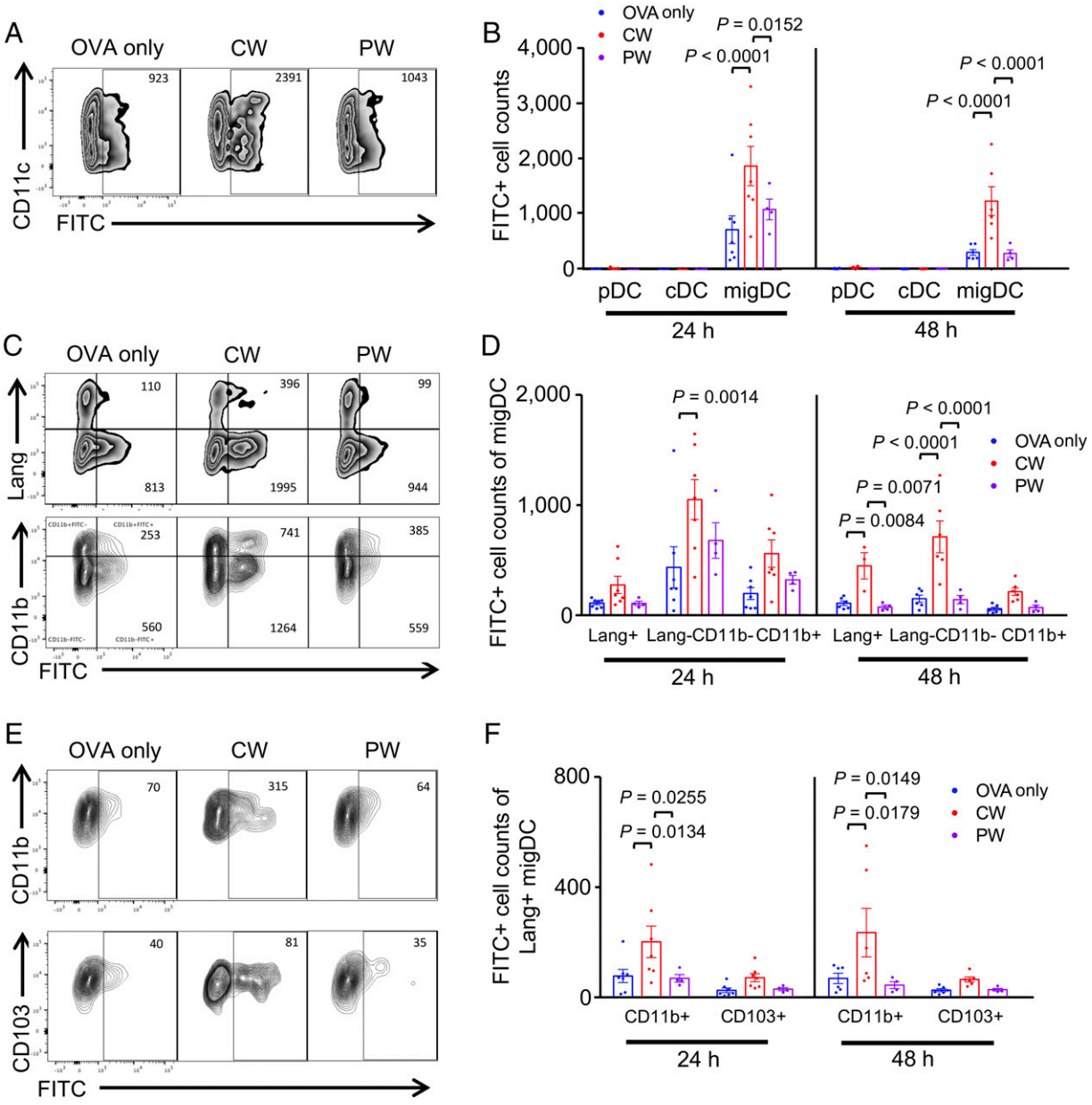

FIGURE 4. The effect of NIR laser on emigration of migDC subsets. Mice were shaved, depilated, and painted with 1% FITC solution on the flank skin 4 h before vaccination with 40 μg of OVA with or without NIR laser treatment. At the times indicated, single-cell suspensions from skin-dLN were labeled and analyzed based on surface markers and FITC fluorescence by flow cytometry. (**A**) Representative gates of FITC$^+$ migDC emigrating into the skin-dLN after FITC painting. (**B**) Cell counts in the skin-dLN after FITC painting. (**C**) Representative gates of migDC subsets. (**D**) Cell counts of migDC subpopulation within skin-dLN after FITC painting. (**E**) Representative gates of Lang$^+$migDC subsets. (**F**) Cell counts of Lang$^+$migDC subpopulation within skin-dLN after FITC painting. (B, E, and F) Two-way ANOVA followed by the Tukey honestly significant difference (HSD) tests. Experimental and control groups: n = 6–7, 6–7, 4 for vaccine i.d., vaccine i.d. + CW 1064 nm, vaccine i.d. + PW 1064 nm, respectively. Data are derived from three independent experiments.

sponding immune responses to intradermal vaccination (Fig. 1), these results indicate that the adjuvant effect of the NIR laser is predominantly mediated by migrational responses of migDC subsets in skin.

The effect of the CW NIR laser adjuvant is mediated by coordination between Lang$^+$ and CD11b$^-$Lang$^-$ migDC subsets

Our data suggest that Lang$^+$ migDC subsets play a pivotal role in the adjuvant effect of the NIR lasers. To assess this, we used a genetic mouse model expressing DT receptor under the control of the langerin promoter (Lang-DTR) (28). Lang-DTR mice were injected with DT 24 h before the OVA immunization. We confirmed that a single DT injection efficiently ablated Lang$^+$ migDC up to 48 h after DT administration, whereas lymphoid tissue–resident cDC were relatively intact (Supplemental Fig. 3), consistent with published observations (28).

Interestingly, when the numbers of Lang$^+$ DC were reduced, the CW NIR laser adjuvant did not induce an increase in the migDC (Fig. 5A, 5B) or CD11b$^-$Lang$^-$ migDC population (Fig. 5C, 5D), which was observed in WT mice (Fig. 2A, 2B, 2E, 2F). In mice lacking Lang$^+$ cells, treatment with the CW NIR laser adjuvant significantly reduced the number of cDCs (Fig. 5A, 5B), but did not induce a significant change in cDC subsets (Fig. 5E, 5F). Mice lacking Lang$^+$ cells treated with the PW NIR laser adjuvant induced a significant decrease of the number of cDCs (Fig. 5A, 5B), a slight decrease of the number of Lang$^-$CD11b$^-$ and CD11b$^+$

migDCs (Fig. 5C, 5D), and no other DC populations changed as compared with OVA i.d. group (Fig. 5A–F).

Deletion of specific DC subsets alters the impact of the NIR laser adjuvant on humoral and cellular responses to influenza vaccination

Our data indicate that the NIR laser adjuvant modulates migDC in skin and induces recruitment of $CD11b^+Ly6C^+$ monocytes. In our previous findings describing the CW NIR laser adjuvant, NIR laser illumination on the skin resulted in increased *ccr7*, *ccl2*, and *ccr2* gene expression and an increase in number of MHC class II^+ $CD11c^+$ DCs within the dLN 6 h after skin illumination with the laser (4). To probe the contribution of specific DC subsets to the efficacy of the NIR laser adjuvant, we took advantage of genetic mouse models in which we can manipulate specific DC subsets in the context of an established model of influenza vaccination. To this end, we evaluated the response of CCR2 deficient ($CCR2^{-/-}$) mice to test the contribution of $CCR2^+$ cells to NIR laser adjuvant response. A CCR2 knockout mice ($CCR2^{-/-}$) model was used to test the contribution of inflammatory monocytes and monocyte-derived DC (16, 37, 38) to the NIR laser adjuvant effect. CCR7-deficient ($CCR7^{-/-}$) mice were also included as a control in these experiments. CCR7 loss entirely inhibits migDC trafficking and has been reported to delay Ab production by B cells (40–42).

The $CCR2^{-/-}$ mice produced generally higher anti-influenza IgG, IgG1, and IgG2c Ab titers than WT mice, with a statistically significant increase observed in anti-influenza IgG1 (WT versus $CCR2^{-/-}$ in i.d. only group: $p = 0.0003$, in PW NIR laser group: $p = 0.0044$, Fig. 6A–C). The CW NIR laser adjuvant induced an increase in anti-influenza IgG and IgG2c compared with i.d. only group in WT mice (Fig. 1A–C), but removal of $CCR2^+$ cells abolished the adjuvant effect of the CW NIR laser to increase anti-influenza IgG and IgG2c responses (Fig. 6A–C). Moreover, this general increase in binding Ab did not lead to a productive neutralizing Ab response as HAI titers in $CCR2^{-/-}$ mice were significantly lower than those in WT mice (WT versus $CCR2^{-/-}$ in i.d. only group: $p = 0.0043$, WT versus $CCR2^{-/-}$ in CW NIR laser group: $p = 0.0043$, Fig. 6D). The mean values of the IgG2c:IgG1 ratio in $CCR2^{-/-}$ mice showed a significant decrease compared with those of WT mice (WT versus $CCR2^{-/-}$: $p = 0.0007$, Fig. 6E). In agreement with the heightened T_H2 response, we observed that the ablation of $CCR2^+$ cells strikingly increases total influenza IL-4 responses, although maintains the same IFN-γ responses (IL-4 of WT versus $CCR2^{-/-}$: $p < 0.0001$, Fig. 6F, 6G). It appears that in the absence of $CCR2^+$ cells, intradermal influenza vaccination produces a heavily T_H2-skewed response, and a balanced response against influenza vaccination requires $CCR2^+$ cells for a productive neutralizing Ab response. These results are consistent with the published finding that $CCR2^+$ inflammatory DCs have the ability to activate $CD4^+$ T cells and drive their polarization toward T_H1 immune responses (38).

As predicted, mice lacking CCR7-dependent migration and receiving an i.d. influenza vaccine showed a significant reduction of anti-influenza IgG (WT versus $CCR7^{-/-}$ in i.d. only group: $p < 0.0001$, WT versus $CCR7^{-/-}$ in CW NIR laser group: $p < 0.0001$, WT versus $CCR7^{-/-}$ in PW NIR laser group: $p = 0.0084$, Fig. 6A), IgG1 (WT versus $CCR7^{-/-}$ in CW NIR laser group: $p = 0.0059$, Fig. 6B), and IgG2c (WT versus $CCR7^{-/-}$ in i.d. only group: $p < 0.0001$, WT versus $CCR7^{-/-}$ in CW NIR laser group: $p < 0.0001$, WT versus $CCR7^{-/-}$ in PW NIR laser group: $p = 0.0088$, Fig. 6C). $CCR7^{-/-}$ mice generally showed a similar IgG2c:IgG1 ratio compared with WT mice (Fig. 6E). Consistent with the significant reduction of anti-influenza Ab response, HAI titers in $CCR7^{-/-}$ mice were significantly lower than those in WT mice (WT versus $CCR7^{-/-}$ in i.d. only group: $p = 0.0030$, Fig. 6D). In addition, IFN-γ influenza-specific splenocyte

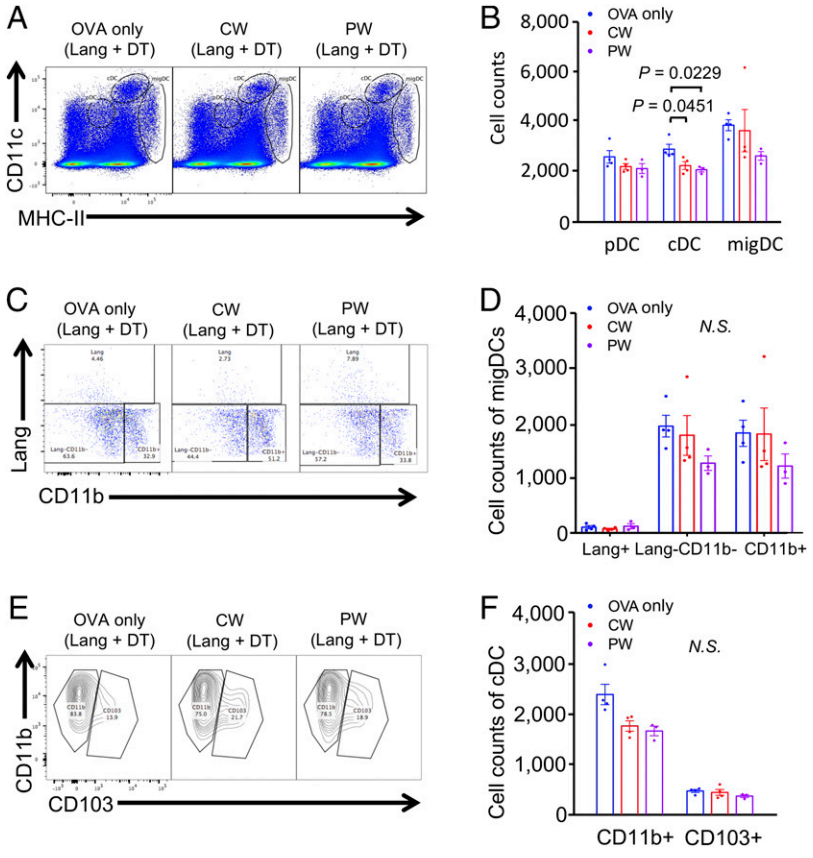

FIGURE 5. Depletion of $Lang^+$ DCs removes CW laser–induced population changes. $Lang^-$DTR/GFP mice were treated with DT 1 d prior to four intradermal injections of 10 μg of A488-labeled OVA with or without laser adjuvant illumination. DCs in skin-dLN were processed and stained for multiparameter flow cytometry 24 h after intradermal vaccination with 40 μg Alexa Fluor-488–labeled OVA with or without 1 min CW or PW 1064 nm NIR laser treatment. (**A**) Representative gates of pDC, cDCs, and migDC; numbers indicate percent of total lymphocytes. (**B**) Cell counts. (**C**) Representative gates of migDC subsets, numbers indicate percent of parent. (**D**) Cell counts of migDC subpopulation within skin-dLN. (**E**) Representative gates of cDC subsets, number indicating percent of parent. (**F**) Cell counts of cDC subpopulation within skin-dLN. (B, D, and F) Data were analyzed with two-way ANOVA followed by Tukey honestly significant difference (HSD) tests. Experimental and control groups: (A–F) $n = 4, 4, 3$ for OVA i.d., OVA i.d. + CW 1064 nm, OVA i.d. + PW 1064 nm, respectively.

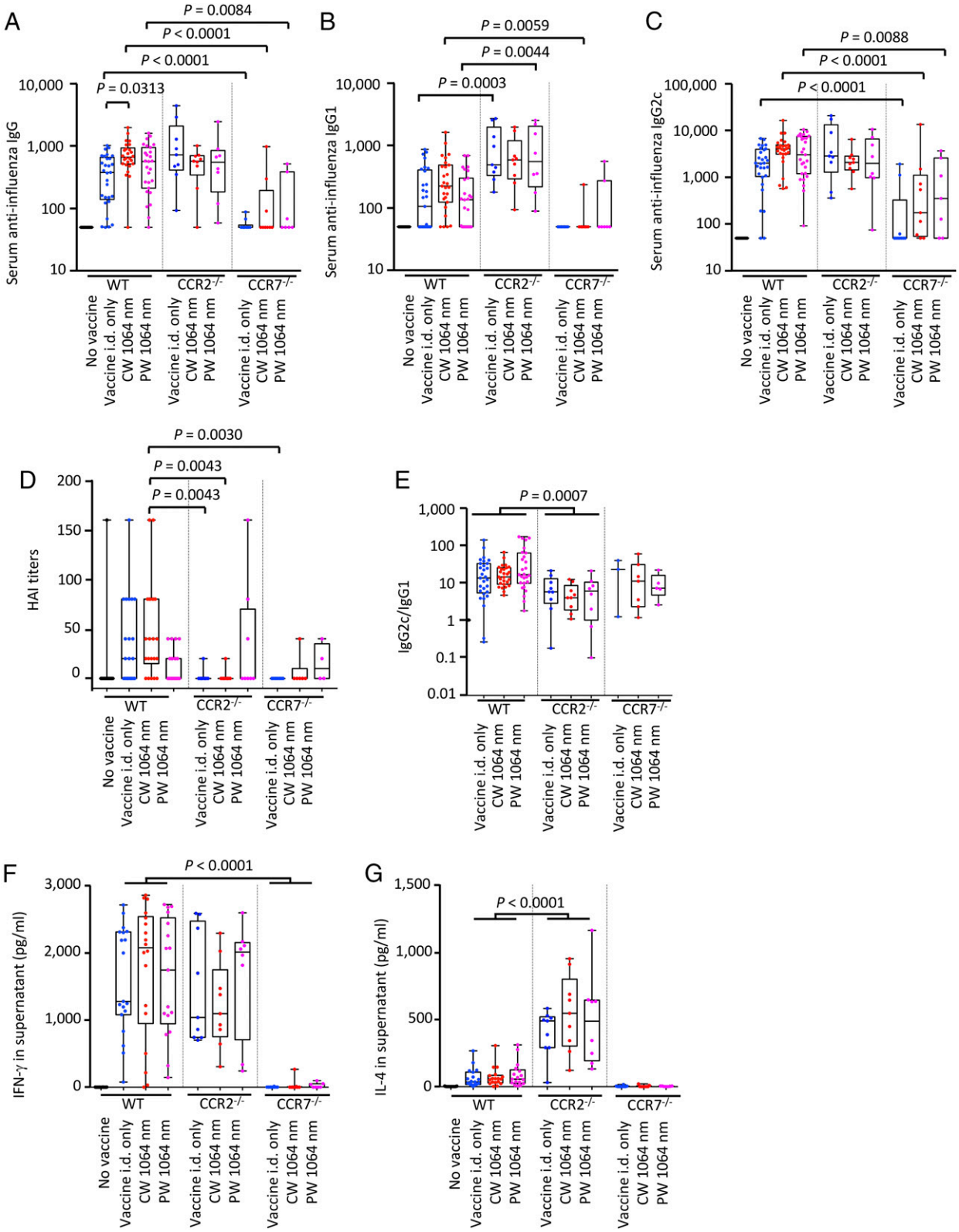

FIGURE 6. Effect of the laser adjuvant on anti-influenza immune responses in CCR2$^{-/-}$ or CCR7$^{-/-}$ mice. (**A**–**E**) Influenza-specific humoral responses in postchallenge (4 d after challenge). C57BL/6 WT, CCR2$^{-/-}$, or CCR7$^{-/-}$ mice were vaccinated with 1 μg of inactivated influenza virus (A/PR/8/34) with or without laser illumination, and challenged intranasally with live homologous virus 4 wk after vaccination. Titer of influenza-specific serum IgG subclass was determined by ELISA. (A) IgG, (B) IgG1, and (C) IgG2c titers. (D) HAI titers. (E) IgG2c/IgG1 ratio. All experiments were repeated three times and pooled to show results. (**F** and **G**) Systemic T cell responses were measured 4 d after challenge by restimulating 1×10^6 splenocytes with inactivated influenza vaccine Ag for 60 h. Levels of (F) IFN-γ and (G) IL-4 in splenocyte culture supernatants are shown. Data were analyzed with two-way ANOVA followed by Tukey honestly significant difference (HSD) tests. WT data from Fig. 1 are shown for comparison. See the *Materials and Methods* section for strategy used for statistical analysis. Experimental and control groups: (A–C and E) $n = 30, 29, 26, 27, 9, 9, 8, 10, 9, 7$; (D) 14, 22, 22, 22, 9, 9, 8, 7, 6, 4; (F and G) $n = 20, 19, 18, 17, 9, 9, 8, 10, 9, 7$ for no vaccine in WT, vaccine i.d. in WT, vaccine i.d. + CW 1064 nm in WT, vaccine i.d. + PW 1064 nm in WT, vaccine i.d. in CCR2$^{-/-}$, vaccine i.d. + CW 1064 nm in CCR2$^{-/-}$, vaccine i.d. + PW 1064 nm in CCR2$^{-/-}$, vaccine i.d. in CCR7$^{-/-}$, vaccine i.d. + CW 1064 nm in CCR7$^{-/-}$, vaccine i.d. + PW 1064 nm in CCR7$^{-/-}$ groups, respectively.

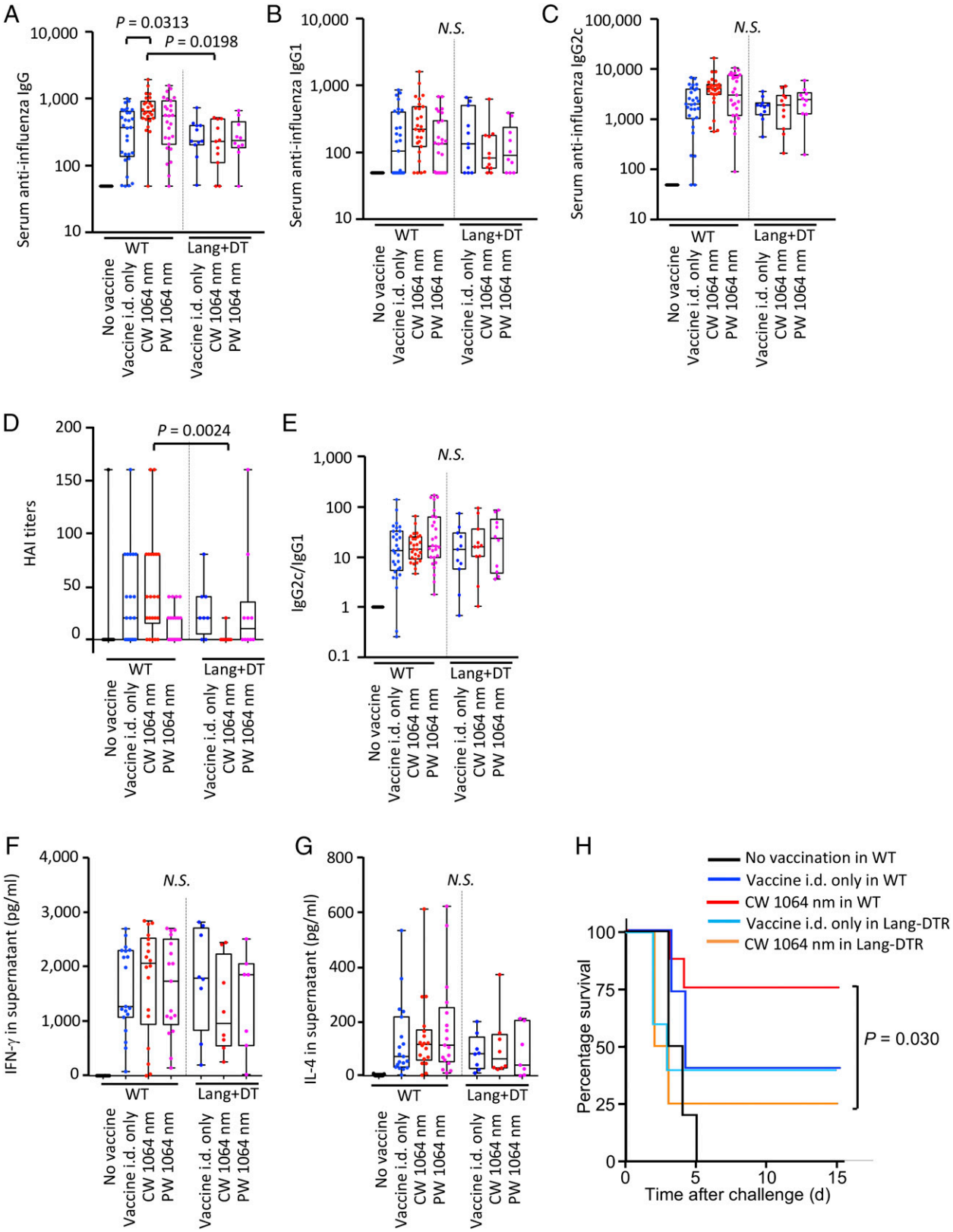

FIGURE 7. Effect of the laser adjuvant on anti-influenza immune responses in Lang$^+$ cell–depleted mice. (**A**–**E**) Influenza-specific humoral responses in postchallenge (4 d after challenge). Lang-DTR/GFP mice were treated with DT 1 d prior to vaccination with 1 μg of inactivated influenza virus (A/PR/8/34) with or without laser illumination and challenged intranasally with live homologous virus 4 wk after vaccination. Titer of influenza-specific serum IgG subclass was determined by ELISA. (A) IgG, (B) IgG1, and (C) IgG2c titers. (D) HAI titers. (E) IgG2c/IgG1 ratio. All experiments were repeated three times and pooled to show results. (**F** and **G**) Systemic T cell responses were measured 4 d after challenge by restimulating 1×10^6 splenocytes with inactivated influenza vaccine Ag for 60 h. Levels of (F) IFN-γ and (G) IL-4 in splenocyte culture supernatants are shown. Data were analyzed with two-way ANOVA followed by Tukey honestly significant difference (HSD) tests. WT data from Fig. 1 are shown for comparison. See the *Materials and Methods* section for strategy used for statistical analysis. Experimental and control groups: (A–C and E) n = 30, 29, 26, 27, 11, 11, 10; (D) n = 14, 22, 22, 22, 8, 11, 10; (F and G) n = 20, 19, 18, 17, 8, 8, 7 for no vaccine in WT, vaccine i.d. in WT, vaccine i.d. + CW 1064 nm in WT, vaccine i.d. + PW 1064 nm (*Figure legend continues*)

responses were significantly reduced as compared with WT mice ($p < 0.0001$, Fig. 6F). CCR7-deficient mice have been reported to lack primary B and T cell responses, showing severely delayed kinetics of the Ab response (42). However, in previously published, reports the humoral response to vaccination eventually reached a similar level to that of WT mice over time. In this study $CCR7^{-/-}$ mice failed to mount significant humoral and cell-mediated immune responses to intradermal vaccination 5 wk after the primary vaccination, which may further support dependence on migratory cells, including migDC. These data build on those provided above by the FITC painting, which consistently show that the effect of the NIR laser is mediated by migrational responses of migDC subsets in skin (Fig. 4). Taken together, these data support the view that the NIR laser adjuvant modulates the migDC in coordination with $CCR2^+$ inflammatory monocytes in the context of intradermal influenza vaccination.

The NIR laser adjuvant depends on the function of $Lang^+$ DC and inflammatory DCs

To assess the functional contribution of each DC subset, we used a genetic mouse model expressing a DTR under the control of the langerin promoter (Lang-DTR). Lang-DTR/GFP mice injected with DT were used to evaluate the immune function of Langerhans cells and $Lang^+$ dermal DCs (28, 43–45).

Depletion of $Lang^+$ cells via DT injection 24 h before the vaccination abolished the effect of the CW NIR laser adjuvants on anti-influenza IgG and IgG2c responses (Fig. 7A–C) and notably decreased IgG response (WT versus Lang/DTR + DT in the CW NIR laser group: $p = 0.0313$, Fig. 7A). Depletion of $Lang^+$ cells consistently and significantly decreased HAI titers in the CW NIR laser group (WT versus Lang/DTR + DT in CW NIR laser group: $p = 0.0024$), but the response in the PW NIR laser group was not affected (Fig. 7D). The IgG2:IgG1 ratio was not significantly changed in any group (Fig. 7E). Depletion of $Lang^+$ cells resulted in a notable decrease in IFN-γ response in CW NIR laser group (Fig. 7F, 7G), although the decrease was not statistically significant.

We next assessed the contribution of $Lang^+$ cells modulated by the NIR laser adjuvant to protection against lethal influenza virus challenge. WT and Lang-DTR mice were vaccinated 24 h after the DT injection with or without the CW NIR laser treatment. Mice were subsequently challenged intranasally with homologous live influenza virus and monitored for survival time. Consistent with our previous study (4), the CW NIR laser treatment consistently conferred better protection compared with no-laser vaccine i.d. only control group (Fig. 7H). In contrast, depletion of $Lang^+$ cells upon vaccination abolished the beneficial effect of the CW NIR laser in Lang-DTR mice (WT versus Lang/DTR in CW NIR laser group: $p = 0.030$, Fig. 7H) with greater weight loss (Supplemental Fig. 4) upon viral challenge. These data support the view that $Lang^+$ cells are necessary for the adjuvant effect of the CW NIR laser.

Thus, our results support the view that $Lang^+$ cells are needed for the CW NIR laser adjuvant effect in the context of intradermal influenza vaccination.

Discussion

In this study, to our knowledge we showed for the first time that the NIR laser adjuvant modulates migDC in the skin and, in the context of intradermal influenza vaccination, adjuvanting effects functionally depend on DC subsets expressing CCR2 and Langerin/CD207. We also found a fundamental difference between the adjuvant effect of CW and PW NIR lasers. The adjuvant effect of the CW NIR laser was shown to be mediated by the coordinated expansion and activation of $Lang^-CD11b^-$ migDC in the presence of $Lang^+$ migDCs and $CCR2^+$ inflammatory monocytes, whereas the PW NIR adjuvant shows a limited effect on $Lang^+$ and $CD11b^+$ migDCs. Our results show that the CW NIR laser adjuvant ultimately induced a mixed T_H1–T_H2 response likely as a result of collaboration among multiple DC subpopulations in skin. In the past decades, multiple phenotypically and functionally distinct DC subsets in the skin have been described. $Lang^+CD103^+$ and $CD11b^+$ DCs have been demonstrated to promote distinct T_H1 and T_H2 responses, respectively (39), and $CCR2^+$ inflammatory monocytes are known to be capable of inducing T_H1 or T_H2 response (16). The CW NIR laser adjuvant requires $CCR2^+$ inflammatory monocytes, which are likely responsible for the induction of a mixed T_H1–T_H2 response. In contrast, the expansion of $CD11b^-Lang^-$ and functional dependence on $Lang^+$ migDC could have contributed to the net difference in productive immunity between the CW and PW NIR laser adjuvant. This double-negative $CD11b^-Lang^-$ migDC subset is less well characterized due to the lack of research tools specifically targeting this subpopulation (39). It has been shown that the $CD11b^-Lang^-$ migDC subpopulation is a bona fide Flt3 ligand–dependent DC, which by transcriptome analysis likely branches from a common precursor with $Lang^-CD11b^+$ migDCs, capable of cross-presentation ex vivo, transports FITC, and is important to the cutaneous immune environment (34), suggesting it has an important role in immune protection in the context of vaccination. In accordance, it has been demonstrated to share transcriptional dependence with $CD11b^-$ migDCs on KLF4 and to regulate T_H2 immunity (46). Further investigation of the significance of $CD11b^-Lang^-$ migDC subset in skin vaccination and protective immunity in the context of the NIR CW laser adjuvant is warranted.

Our results support the clear advantage of the NIR laser adjuvant over chemical vaccine adjuvants approved for intradermal vaccination. Conventional chemicals or biologics are designed to trigger a danger signal to the innate immunity to enhance the immune response to vaccine Ags (47, 48). Amplification of innate immunity typically involves persistent inflammatory responses that are intrinsically linked to the reactogenic and toxic effects of adjuvants (31, 49, 50). In contrast to this, we found that the NIR laser adjuvant possesses a unique ability to selectively modulate specific DC populations in skin, depending on the laser parameter, without inducing apparent inflammation. A broad range of transdermal and intradermal vaccination technologies (51, 52) would benefit from the inclusion of an adjuvant, but use of conventional chemical or biological adjuvants in the confines of the skin results in unacceptable inflammatory responses (53, 54). Consequently, only a small number of proposed adjuvants are ideally suited for use in the skin (55, 56). In the current study, both of the representative clinical adjuvants, alum and AddaVax, (an oil-in-water emulsion adjuvant with a formulation similar to MF59), induced significant upregulation of influenza-specific IgE in the context of intradermal influenza vaccination (Fig. 1F), which may lead to an

in WT, vaccine i.d. in Lang/DTR + DT, vaccine i.d. + CW 1064 nm in Lang/DTR + DT, vaccine i.d. + PW 1064 nm in Lang/DTR + DT groups, respectively. (**H**) Kaplan–Meier survival plots of influenza-vaccinated mice for 15 d following lethal challenge. Data were analyzed with Gehan–Breslow–Wilcoxon test. EID_{50}, the 50% egg infectious dose. Experimental and control groups: $n = 10, 15, 8, 5, 4$ for no vaccine in WT, vaccine i.d. in WT, vaccine i.d. + CW 1064 nm in WT, vaccine i.d. in Lang/DTR + DT, vaccine i.d. + CW 1064 nm in Lang/DTR + DT, respectively.

adverse response induced by vaccination. In contrast, the NIR laser adjuvant did not induce an IgE response to intradermal vaccination. Our previous study showed that the NIR laser adjuvant induces selective cellular signaling without inducing apparent tissue inflammation (4, 25). The current study further demonstrates that the NIR laser adjuvant is able to selectively modulate the most versatile and important cell population to augment adaptive immune responses, namely migDC, without inducing adverse IgE responses. These results show distinct mechanisms of action of the NIR laser compared with conventional vaccine adjuvants, highlighting a novel possibility of reproducible control over the immune response by a physical parameter for desirable protection with an intradermal vaccine.

Investigators have established that heterogeneous DC populations found in the skin cover a broad array of functions, from inducing protection against various pathogens to maintaining peripheral tolerance (39). It is becoming increasingly evident that specialized DC subsets can exert specific functions, but these functions are often defined by the cues the DC receives from its microenvironment (57, 58). Hence, the induction of the immune response should be considered the result of balanced expansion and activation of specialized DC subsets and environmental cues. Because our results show that the CW or PW NIR laser evoked distinct immunological events, each NIR laser adjuvant appears able to provide immunostimulatory cues unique to its laser parameters in skin. Although the precise molecular signaling involved in this process has yet to be explored, our previous and current studies have shown that the NIR laser adjuvant is nondamaging to the tissue and does not induce typical inflammatory responses, but rather selective innate signaling including temporal upregulation of a selective set of chemokines that enhances the activation and recruitment of APCs in the skin (4). Onikienko et al. (59) identified an important role of release of intracellular Hsp70 into the extracellular space in skin tissue in nanosecond-pulsed high-frequency laser adjuvant, thereby inducing T_H1 response via the TLR4 receptor (5, 6). Heat shock proteins expressed on the surface of stressed and damaged cells can serve as a type of danger signal and are recognized by APCs through specific receptors, such as TLRs and scavenger receptors resulting in priming T cells (60, 61).

In addition, a thermal mechanism does not appear to mediate the impact of the NIR laser on the immune system. Laser light is absorbed by skin chromophores depending on its wavelength and generates heat in the skin. Although the thermal profile of PW 1064 nm laser in skin is equivalent to that of the CW 1064 nm laser (4), the current study shows that these lasers evoked quite distinct effects on the adaptive immune response and DC subsets in skin. Therefore, we believe the thermal effect plays a minimal role in the adjuvant effect of the NIR lasers. In this study, we have shown the possible link between cues induced by the CW NIR laser and the enrichment of $CD11b^{-}Lang^{-}$ migDC and functional dependence on $Lang^{+}$ migDC, while demonstrating that cues induced by the PW NIR laser led to limited modulation of $Lang^{+}$ and $CD11b^{+}$ migDCs. The precise relationship between molecular cues and their interactions with specific migDC subpopulations need to be further characterized in future studies for the optimization of the NIR laser adjuvant.

In summary, the NIR laser adjuvant possesses the unique ability to selectively target specific DC subsets in skin and could offer protection by an NIR laser–adjuvanted vaccine depending on its laser parameters in the context of intradermal vaccination. These findings boost efforts to customize the combination of intradermal vaccines with the laser adjuvant for the induction of immune protection from pathogens.

Acknowledgments

We thank Dr. Hang Lee, a consultant for the Harvard Catalyst Bio-Statistical Consulting Group, for statistical analysis. We also thank Madeline Penson for excellent technical assistance, and Susan Raju Paul and Patrick Reeves (all at the Vaccine and Immunotherapy Center, Massachusetts General Hospital) for fruitful discussions.

Disclosures

The authors have no financial conflicts of interest.

References

1. Batista-Duharte, A., E. B. Lindblad, and E. Oviedo-Orta. 2011. Progress in understanding adjuvant immunotoxicity mechanisms. *Toxicol. Lett.* 203: 97–105.
2. Lee, S., and M. T. Nguyen. 2015. Recent advances of vaccine adjuvants for infectious diseases. *Immune Netw.* 15: 51–57.
3. Rappuoli, R., C. W. Mandl, S. Black, and E. De Gregorio. 2011. Vaccines for the twenty-first century society. *Nat. Rev. Immunol.* 11: 865–872.
4. Kashiwagi, S., J. Yuan, B. Forbes, M. L. Hibert, E. L. Lee, L. Whicher, C. Goudie, Y. Yang, T. Chen, B. Edelblute, et al. 2013. Near-infrared laser adjuvant for influenza vaccine. *PLoS One* 8: e82899.
5. Kashiwagi, S., T. Brauns, J. Gelfand, and M. C. Poznansky. 2014. Laser vaccine adjuvants. History, progress, and potential. *Hum. Vaccin. Immunother.* 10: 1892–1907.
6. Kashiwagi, S., T. Brauns, and M. C. Poznansky. 2016. Classification of laser vaccine adjuvants. *J. Vaccines Vaccin.* 7: 307.
7. Awate, S., L. A. Babiuk, and G. Mutwiri. 2013. Mechanisms of action of adjuvants. *Front. Immunol.* 4: 114.
8. Coffman, R. L., A. Sher, and R. A. Seder. 2010. Vaccine adjuvants: putting innate immunity to work. *Immunity* 33: 492–503.
9. Steinman, R. M. 2008. Dendritic cells in vivo: a key target for a new vaccine science. *Immunity* 29: 319–324.
10. Boscardin, S. B., J. C. Hafalla, R. F. Masilamani, A. O. Kamphorst, H. A. Zebroski, U. Rai, A. Morrot, F. Zavala, R. M. Steinman, R. S. Nussenzweig, and M. C. Nussenzweig. 2006. Antigen targeting to dendritic cells elicits long-lived T cell help for antibody responses. *J. Exp. Med.* 203: 599–606.
11. Steinman, R. M., and J. Banchereau. 2007. Taking dendritic cells into medicine. *Nature* 449: 419–426.
12. Mora, J. R., G. Cheng, D. Picarella, M. Briskin, N. Buchanan, and U. H. von Andrian. 2005. Reciprocal and dynamic control of CD8 T cell homing by dendritic cells from skin- and gut-associated lymphoid tissues. *J. Exp. Med.* 201: 303–316.
13. Klechevsky, E., R. Morita, M. Liu, Y. Cao, S. Coquery, L. Thompson-Snipes, F. Briere, D. Chaussabel, G. Zurawski, A. K. Palucka, et al. 2008. Functional specializations of human epidermal Langerhans cells and CD14+ dermal dendritic cells. *Immunity* 29: 497–510.
14. Devi, K. S., and N. Anandasabapathy. 2017. The origin of DCs and capacity for immunologic tolerance in central and peripheral tissues. *Semin. Immunopathol.* 39: 137–152.
15. Nirschl, C. J., and N. Anandasabapathy. 2016. Duality at the gate: skin dendritic cells as mediators of vaccine immunity and tolerance. *Hum. Vaccin. Immunother.* 12: 104–116.
16. Segura, E., and S. Amigorena. 2013. Inflammatory dendritic cells in mice and humans. *Trends Immunol.* 34: 440–445.
17. Schlitzer, A., N. McGovern, and F. Ginhoux. 2015. Dendritic cells and monocyte-derived cells: two complementary and integrated functional systems. *Semin. Cell Dev. Biol.* 41: 9–22.
18. Merad, M., F. Ginhoux, and M. Collin. 2008. Origin, homeostasis and function of Langerhans cells and other langerin-expressing dendritic cells. *Nat. Rev. Immunol.* 8: 935–947.
19. López-Bravo, M., and C. Ardavín. 2008. In vivo induction of immune responses to pathogens by conventional dendritic cells. *Immunity* 29: 343–351.
20. Merad, M., P. Sathe, J. Helft, J. Miller, and A. Mortha. 2013. The dendritic cell lineage: ontogeny and function of dendritic cells and their subsets in the steady state and the inflamed setting. *Annu. Rev. Immunol.* 31: 563–604.
21. Guilliams, M., P. Bruhns, Y. Saeys, H. Hammad, and B. N. Lambrecht. 2014. The function of Fcγ receptors in dendritic cells and macrophages. *Nat. Rev. Immunol.* 14: 94–108.
22. Wang, J., B. Li, and M. X. Wu. 2015. Effective and lesion-free cutaneous influenza vaccination. *Proc. Natl. Acad. Sci. USA* 112: 5005–5010.
23. Wang, J., D. Shah, X. Chen, R. R. Anderson, and M. X. Wu. 2014. A microsterile inflammation array as an adjuvant for influenza vaccines. *Nat. Commun.* 5: 4447.
24. Terhorst, D., R. Chelbi, C. Wohn, C. Malosse, S. Tamoutounour, A. Jorquera, M. Bajenoff, M. Dalod, B. Malissen, and S. Henri. 2015. Dynamics and transcriptomics of skin dendritic cells and macrophages in an imiquimod-induced, biphasic mouse model of psoriasis. *J. Immunol.* 195: 4953–4961.
25. Kimizuka, Y., J. J. Callahan, Z. Huang, K. Morse, W. Katagiri, A. Shigeta, R. Bronson, S. Takeuchi, Y. Shimaoka, M. P. Chan, et al. 2017. Semiconductor diode laser device adjuvanting intradermal vaccine. *Vaccine* 35: 2404–2412.

26. Chen, X., P. Kim, B. Farinelli, A. Doukas, S. H. Yun, J. A. Gelfand, R. R. Anderson, and M. X. Wu. 2010. A novel laser vaccine adjuvant increases the motility of antigen presenting cells. *PLoS One* 5: e13776.
27. Jung, S., D. Unutmaz, P. Wong, G. Sano, K. De los Santos, T. Sparwasser, S. Wu, S. Vuthoori, K. Ko, F. Zavala, et al. 2002. In vivo depletion of CD11c+ dendritic cells abrogates priming of CD8+ T cells by exogenous cell-associated antigens. *Immunity* 17: 211–220.
28. Kissenpfennig, A., S. Henri, B. Dubois, C. Laplace-Builhé, P. Perrin, N. Romani, C. H. Tripp, P. Douillard, L. Leserman, D. Kaiserlian, et al. 2005. Dynamics and function of Langerhans cells in vivo: dermal dendritic cells colonize lymph node areas distinct from slower migrating Langerhans cells. *Immunity* 22: 643–654.
29. Anandasabapathy, N., R. Feder, S. Mollah, S. W. Tse, M. P. Longhi, S. Mehandru, I. Matos, C. Cheong, D. Ruane, L. Brane, et al. 2014. Classical Flt3L-dependent dendritic cells control immunity to protein vaccine. *J. Exp. Med.* 211: 1875–1891.
30. Macatonia, S. E., S. C. Knight, A. J. Edwards, S. Griffiths, and P. Fryer. 1987. Localization of antigen on lymph node dendritic cells after exposure to the contact sensitizer fluorescein isothiocyanate. Functional and morphological studies. *J. Exp. Med.* 166: 1654–1667.
31. Gupta, R. K., B. E. Rost, E. Relyveld, and G. R. Siber. 1995. Adjuvant properties of aluminum and calcium compounds. *Pharm. Biotechnol.* 6: 229–248.
32. Henri, S., M. Guilliams, L. F. Poulin, S. Tamoutounour, L. Ardouin, M. Dalod, and B. Malissen. 2010. Disentangling the complexity of the skin dendritic cell network. *Immunol. Cell Biol.* 88: 366–375.
33. Poulin, L. F., S. Henri, B. de Bovis, E. Devilard, A. Kissenpfennig, and B. Malissen. 2007. The dermis contains langerin+ dendritic cells that develop and function independently of epidermal Langerhans cells. *J. Exp. Med.* 204: 3119–3131.
34. Mollah, S. A., J. S. Dobrin, R. E. Feder, S. W. Tse, I. G. Matos, C. Cheong, R. M. Steinman, and N. Anandasabapathy. 2014. Flt3L dependence helps define an uncharacterized subset of murine cutaneous dendritic cells. *J. Invest. Dermatol.* 134: 1265–1275.
35. Guilliams, M., C. A. Dutertre, C. L. Scott, N. McGovern, D. Sichien, S. Chakarov, S. Van Gassen, J. Chen, M. Poidinger, S. De Prijck, et al. 2016. Unsupervised high-dimensional analysis aligns dendritic cells across tissues and species. *Immunity* 45: 669–684.
36. Reizis, B., M. Colonna, G. Trinchieri, F. Barrat, and M. Gilliet. 2011. Plasmacytoid dendritic cells: one-trick ponies or workhorses of the immune system? *Nat. Rev. Immunol.* 11: 558–565.
37. Boring, L., J. Gosling, S. W. Chensue, S. L. Kunkel, R. V. Farese, Jr., H. E. Broxmeyer, and I. F. Charo. 1997. Impaired monocyte migration and reduced type 1 (Th1) cytokine responses in C-C chemokine receptor 2 knockout mice. *J. Clin. Invest.* 100: 2552–2561.
38. Nakano, H., K. L. Lin, M. Yanagita, C. Charbonneau, D. N. Cook, T. Kakiuchi, and M. D. Gunn. 2009. Blood-derived inflammatory dendritic cells in lymph nodes stimulate acute T helper type 1 immune responses. *Nat. Immunol.* 10: 394–402.
39. Malissen, B., S. Tamoutounour, and S. Henri. 2014. The origins and functions of dendritic cells and macrophages in the skin. *Nat. Rev. Immunol.* 14: 417–428.
40. Villablanca, E. J., and J. R. Mora. 2008. A two-step model for Langerhans cell migration to skin-draining LN. *Eur. J. Immunol.* 38: 2975–2980.
41. Ohl, L., M. Mohaupt, N. Czeloth, G. Hintzen, Z. Kiafard, J. Zwirner, T. Blankenstein, G. Henning, and R. Förster. 2004. CCR7 governs skin dendritic cell migration under inflammatory and steady-state conditions. *Immunity* 21: 279–288.
42. Förster, R., A. Schubel, D. Breitfeld, E. Kremmer, I. Renner-Müller, E. Wolf, and M. Lipp. 1999. CCR7 coordinates the primary immune response by establishing functional microenvironments in secondary lymphoid organs. *Cell* 99: 23–33.
43. Bennett, C. L., M. Noordegraaf, C. A. Martina, and B. E. Clausen. 2007. Langerhans cells are required for efficient presentation of topically applied hapten to T cells. *J. Immunol.* 179: 6830–6835.
44. Clausen, B. E., and J. M. Kel. 2010. Langerhans cells: critical regulators of skin immunity? *Immunol. Cell Biol.* 88: 351–360.
45. Kaplan, D. H., A. Kissenpfennig, and B. E. Clausen. 2008. Insights into Langerhans cell function from Langerhans cell ablation models. *Eur. J. Immunol.* 38: 2369–2376.
46. Tussiwand, R., B. Everts, G. E. Grajales-Reyes, N. M. Kretzer, A. Iwata, J. Bagaitkar, X. Wu, R. Wong, D. A. Anderson, T. L. Murphy, et al. 2015. Klf4 expression in conventional dendritic cells is required for T helper 2 cell responses. *Immunity* 42: 916–928.
47. Matzinger, P. 2002. The danger model: a renewed sense of self. *Science* 296: 301–305.
48. Petrovsky, N. 2008. Freeing vaccine adjuvants from dangerous immunological dogma. *Expert Rev. Vaccines* 7: 7–10.
49. Israeli, E., N. Agmon-Levin, M. Blank, and Y. Shoenfeld. 2009. Adjuvants and autoimmunity. *Lupus* 18: 1217–1225.
50. Cruz-Tapias, P., N. Agmon-Levin, E. Israeli, J. M. Anaya, and Y. Shoenfeld. 2013. Autoimmune (auto-inflammatory) syndrome induced by adjuvants (ASIA)–animal models as a proof of concept. *Curr. Med. Chem.* 20: 4030–4036.
51. Kim, Y. C., C. Jarrahian, D. Zehrung, S. Mitragotri, and M. R. Prausnitz. 2012. Delivery systems for intradermal vaccination. *Curr. Top. Microbiol. Immunol.* 351: 77–112.
52. Zehrung, D., C. Jarrahian, and A. Wales. 2013. Intradermal delivery for vaccine dose sparing: overview of current issues. *Vaccine* 31: 3392–3395.
53. Chen, X., M. Pravetoni, B. Bhayana, P. R. Pentel, and M. X. Wu. 2012. High immunogenicity of nicotine vaccines obtained by intradermal delivery with safe adjuvants. *Vaccine* 31: 159–164.
54. Vitoriano-Souza, J., Nd. Moreira, A. Teixeira-Carvalho, C. M. Carneiro, F. A. Siqueira, P. M. Vieira, R. C. Giunchetti, S. A. Moura, R. T. Fujiwara, M. N. Melo, and A. B. Reis. 2012. Cell recruitment and cytokines in skin mice sensitized with the vaccine adjuvants: saponin, incomplete Freund's adjuvant, and monophosphoryl lipid A. *PLoS One* 7: e40745.
55. Hu, J. C., C. Mathias-Santos, C. J. Greene, N. D. King-Lyons, J. F. Rodrigues, G. Hajishengallis, L. C. Ferreira, and T. D. Connell. 2014. Intradermal administration of the Type II heat-labile enterotoxins LT-IIb and LT-IIc of enterotoxigenic *Escherichia coli* enhances humoral and CD8+ T cell immunity to a co-administered antigen. *PLoS One* 9: e113978.
56. Mattsson, J., K. Schön, L. Ekman, L. Fahlén-Yrlid, U. Yrlid, and N. Y. Lycke. 2015. Cholera toxin adjuvant promotes a balanced Th1/Th2/Th17 response independently of IL-12 and IL-17 by acting on Gsα in $CD11b^+$ DCs. *Mucosal Immunol.* 8: 815–827.
57. Romani, N., V. Flacher, C. H. Tripp, F. Sparber, S. Ebner, and P. Stoitzner. 2012. Targeting skin dendritic cells to improve intradermal vaccination. *Curr. Top. Microbiol. Immunol.* 351: 113–138.
58. Clausen, B. E., and P. Stoitzner. 2015. Functional specialization of skin dendritic cell subsets in regulating T cell responses. *Front. Immunol.* 6: 534.
59. Onikienko, S. B., A. B. Zemlyanoy, B. A. Margulis, I. V. Guzhova, M. B. Varlashova, V. S. Gornostaev, N. V. Tikhonova, G. A. Baranov, and V. V. Lesnichiy. 2007. Diagnostics and correction of the metabolic and immune disorders. Interactions of bacterial endotoxins and lipophilic xenobiotics with receptors associated with innate immunity. *Donosologiya (St. Petersburg)* 1: 32–54.
60. Segal, B. H., X. Y. Wang, C. G. Dennis, R. Youn, E. A. Repasky, M. H. Manjili, and J. R. Subjeck. 2006. Heat shock proteins as vaccine adjuvants in infections and cancer. *Drug Discov. Today* 11: 534–540.
61. Kono, H., and K. L. Rock. 2008. How dying cells alert the immune system to danger. *Nat. Rev. Immunol.* 8: 279–289.